ChemPubSoc Europe

DOI: 10.1002/slct.201901325

Chemistry SELECT Full Papers

Materials Science inc. Nanomaterials & Polymers

New Insights into the Triton X-100 Induced Chemical Exfoliation of MoS_2 to Derive Highly Luminescent Nanosheets

Garima Kedawat+,[a] Pawan Kumar+,[a] Kanika Nagpal,[a] Sharon J. Paul,[a, b] V. N. Singh,[c] Sampath Satheesh Kumar,[d] and Bipin Kumar Gupta*[a]

The exfoliation of two dimensional (2D) transition metal dichalcogenides (TMDs) into mono- or few-layers without compromising their semiconductor properties has momentous interest for both point of view; fundamental studies and further implementation in practical applications. Herein, we reported a novel and inexpensive approach for high yield nanosheets from bulk MoS_2 to few layers of strong luminescent MoS_2 nanosheets using Triton X-100 as a surfactant with tailoring the bulk band gap 1.2 eV to 1.79 eV of few layers of nanosheets after chemical exfoliation process, which can be easily scaled-up in large quantity. The microstructural results reveal that the exfoliated nanosheets have thickness in the range of few layers and lateral dimension in the range of few hundred nanometers. Our findings may offer a new innovative one setup chemical exfoliation process to design a few layer of MoS_2 nanosheets without suppressing luminescent properties, which is highly desirable for the next generation optoelectronic devices.

Introduction

The two dimensional (2D) transition metal dichalcogenides (TMD) are an emerging class of 2D materials, and they have gained huge attention due to their unique electrical, optical, mechanical, and chemical properties and prospect for a wide range of applications.[1–4] Among the 2D TMDs, the MoS_2 has attracted researchers' significantly due to its excellent properties such as large intrinsic band gap, stiffness, electrical and optical properties.[5] The MoS_2 has a hexagonal structure (2H), where S–Mo-S atoms are arranged in a hexagonal pattern, and these planes are closely packed by interlayer van der Waals interactions.[6] The bulk MoS_2 is an indirect band gap semiconductor with band gap of ~1.2 eV. The bandgap of MoS_2 is increased with a decrease in thickness (below 100 nm). Theoretically, it is predicted that the monolayer of MoS_2 has a direct band gap of ~ 1.9 eV.[2,4] Moreover, the band gap of MoS_2 changes from indirect to direct due to quantum confinement. The indirect to the direct transition of bandgap with decrease in thickness, results in an enhancement in photoluminescence quantum yield, which makes MoS_2 as a potential candidate for advanced optoelectronic devices.

Consequently, the exfoliation of MoS_2 into monolayer and few layers is an important step prior to make it optically active as well as its further execution in potential applications. Additionally, for a scalable production of MoS_2 nanosheets based devices, a facile method is required, which not only provides large-scale synthesis but also an inexpensive method to produce monolayer and few layers of MoS_2. The chemical exfoliation of MoS_2 is a promising route to achieve these goals and its demonstration for practical uses. In recent years, there are many reports on the liquid phase exfoliation of TMDs using different organic solvent.[2,7–9] Coleman et. al. demonstrated the liquid phase exfoliation of various bulk 2D layered compounds such as MoS_2, WS_2, $MoSe_2$, $MoTe_2$, $TaSe_2$, $NbSe_2$, $NiTe_2$, BN, and Bi_2Te_3 into layers in various organic solvents by ultrasonication.[10] Natural bulk MoS_2 has two poly types 2H and 3R, both of them occur in exfoliated state. Moreover unlike the bulk MoS_2, monolayer MoS_2 is a direct band gap material which was confirmed experimentally. Although, there are some reports on the exfoliation of bulk MoS_2 powder into monolayer or few layers in organic solvent with assistance of ultrasonication by intercalation of Li between the layers of MoS_2.[2,11,12] This method of exfoliation offers a versatile route for high yield exfoliated MoS_2 nanosheets but still this method has some drawbacks. One of the major drawbacks of this method is the Li-ions intercalation on surface of MoS_2 layer, which leads to the formation of Li_xMoS_2 layer. The removal of Li ion from the surface of MoS_2 is a very challenging task. Furthermore, the interaction of Li ions is also attributed to the partial phase change in the pristine MoS_2 leading to the change in electrical and optical properties. Since, the intercalation of Li ions (metallic ion) in MoS_2 layers leads to the formation of

[a] Dr. G. Kedawat,+ Dr. P. Kumar,+ K. Nagpal, S. J. Paul, Dr. B. K. Gupta
Photonic Materials Metrology Sub Division, Advanced Materials and Device Metrology Division
CSIR – National Physical Laboratory, New Delhi, India
E-mail: bipinbhu@yahoo.com
[b] S. J. Paul
Bundelkhand University, Jhansi, Uttar Pradesh, 284128, India
[c] Dr. V. N. Singh
In-House BND Sub Division, Bharatiya Nirdeshak Dravyas Division, CSIR – National Physical Laboratory, New Delhi, India
[d] S. S. Kumar
WITec GmbH, Lise-Meitner-Str. 6, D-89081 Ulm, Germany
[+] Both authors have equally contributed.

Supporting information for this article is available on the WWW under https://doi.org/10.1002/slct.201901325

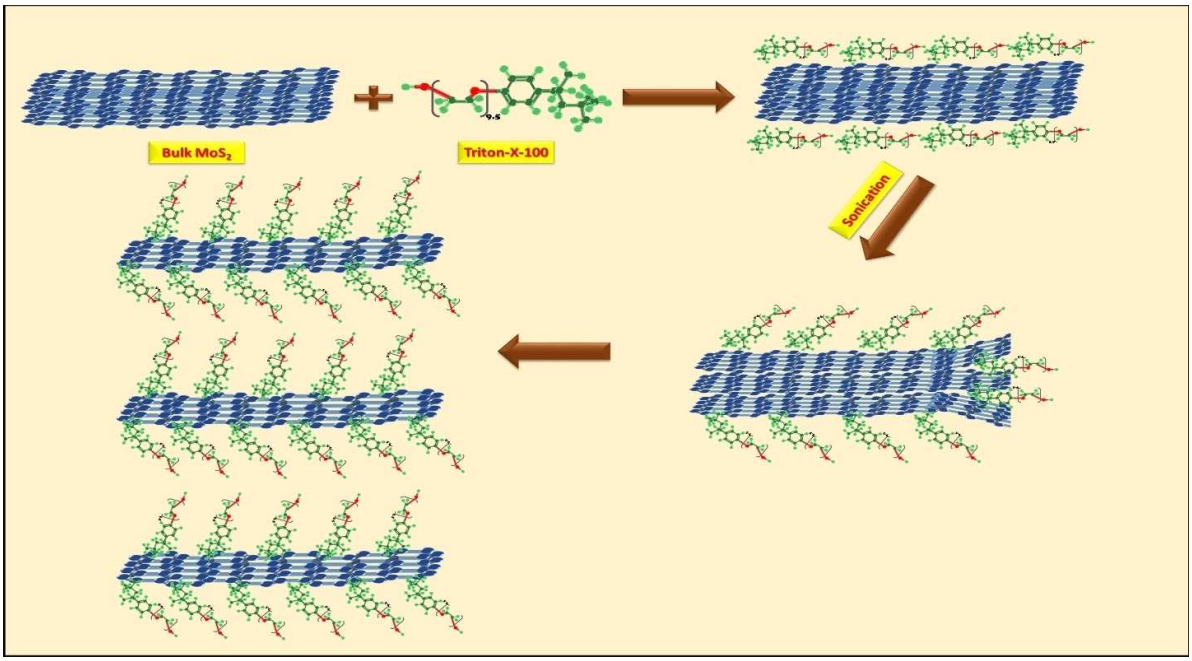

Figure 1. The various steps involved in Triton-X 100 mediated exfoliated MoS_2 nanosheets.

metallic phase, it results in loss of semiconductor properties of MoS_2. However, there are also few reports on liquid phase exfoliation of MoS_2 by using sodium based surfactant but these methods suffer same issue..[13,14] The intercalation of metal ion (Na^+ ion) on the surface of MoS_2 results in loss of semiconductor properties of MoS_2. Therefore, the high yield exfoliation of MoS_2 without compromising the properties of pristine MoS_2 is still a challenging task, which is addressed in the present work.

Herein, we reported a sonication method for chemical exfoliation of MoS_2 in an aqueous solution of Triton X-100. As the ionic and non-ionic surfactant show different colloidal stability, in present study, we have chosen Triton X-100 a non-ionic surfactant. It has a hydrophilic polyethylene oxide group and a lipophilic or hydrophobic group covalently bonded to a centered benzene ring, as well as Triton X-100 has low cost, low toxicity and low boiling point. This surfactant does not contain any metallic ion; consequently it does not affect the semiconductor properties of pristine MoS_2. The Triton X-100 is able to work as dispersing agent and as stabilizer to prevent layer stacking. When the MoS_2 sheets adhere to the Triton X-100 surfactant molecules, which are merely charged, the electrostatic force becomes much lower. Thus, the Triton X-100 surfactant has a unique property as compared to other surfactants. Additionally, some papers are reported on the non-ionic surfactant Triton X-100 induced exfoliation of graphene and TMDs from bulk powder into few layers.[15–17] The use of Triton X-100 is to stabilize graphene and TMDs nanoflakes in solution. This is the major breakthrough to maintain semiconductor properties by using non-ionic surfactants. The main focus of our work is to introduce Triton X-100 as a new surfactant for exfoliation of MoS_2. Additionally, the two-dimensional materials still have numerous challenges that need to be overcome to enable their application in optoelectronics devices. These include improving their poor photoluminescence (PL) as well as better understanding of exciton-based recombination kinetics. Therefore, MoS_2 nanosheets are synthesized from bulk using Triton X-100 as a non-ionic surfactant by chemical exfoliation technique, which improves the PL in MoS_2 nanosheets from bulk in a single stage. In order to understand the quality and luminescent properties of exfoliated MoS_2 nanosheets, we performed specially resolve PL and Raman mapping spectroscopy, which is not reported so far for Triton X-100 induced exfoliation. This facile approach is insensitive to air and can be scaled-up in large quantities at low cost. Thus, Triton X-100 induced liquid phase exfoliation of MoS_2 without compromising the semiconductor properties of pristine MoS_2 may open new opportunities in the development of highly luminescent 2D materials based optoelectronic devices and its potential use in emerging new technologies.

Result and Discussion

The exfoliation of 2D TMDs into mono or few layers have gained significant interest worldwide for both the fundamental studies and potential applications point of view.[8] In present study we have reported for the first time, the surfactant induced exfoliation of bulk MoS_2 using Triton X-100. The plausible mechanism for the Triton X-100 induced exfoliation of MoS_2 bulk powder into nanosheets is illustrated in Figure 1. It shows various processing steps involved in Triton X-100 mediated exfoliation of MoS_2. The bulk MoS_2 and non-ionic surfactant molecules of Triton X-100 were dispersed in DI-water. Initially, the exfoliation of bulk MoS_2 is due to the

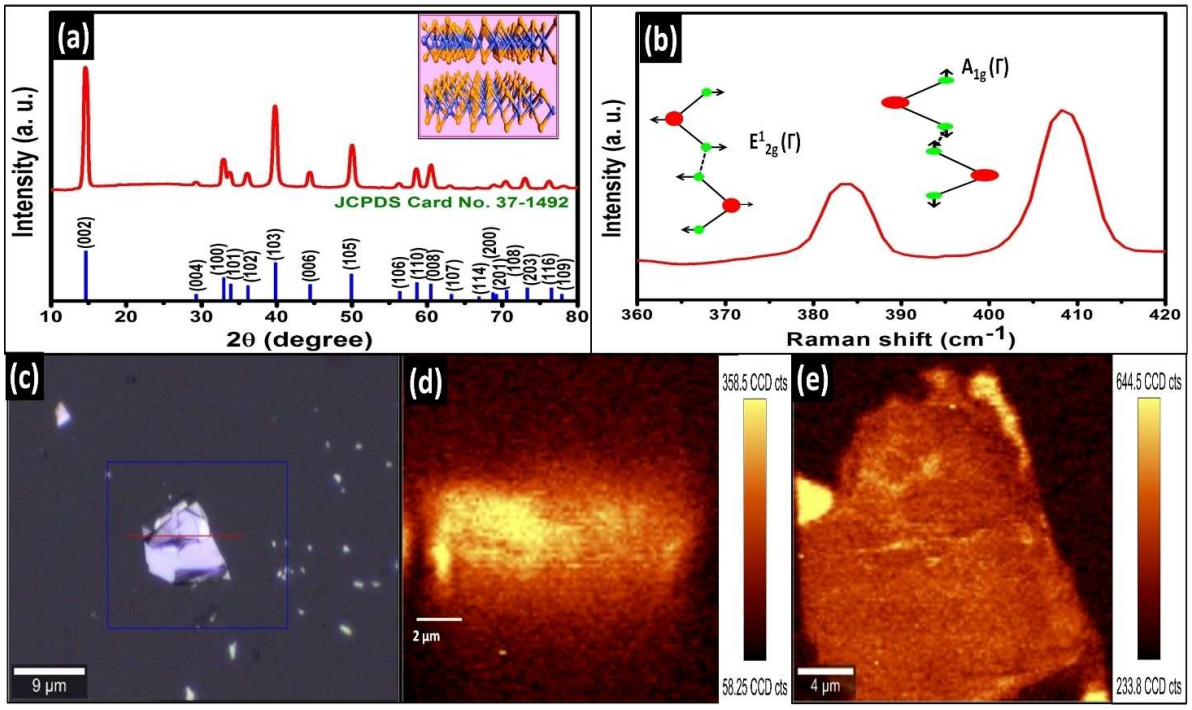

Figure 2. (a) XRD pattern of as-synthesized M1 sample and vertical tick marks below the XRD curve shows the Bragg positions corresponding JCPDS No. 37–1492 and inset shows the schematic of the atomic-layered MoS_2, (b) the enlarge view of raman spectrum; having two prominent peaks, showing a strong in-plane vibrational mode of the Mo and S atoms (E^1_{2g} modes) and the out-of-plane vibrational mode of S atoms (A_{1g} modes), (c) the optical image, (d) optical profile and (e) their corresponding Raman mapping of as synthesized M1 sample; The depth profile (d) and Raman mapping (e) were recorded at spots indicated by red colored straight line and blue colored square in (c), respectively.

introduction of shear force and sonication-derived cavitation i.e. the formation and breakdown of micrometer-sized bubbles or voids in the water due to the pressure fluctuations during ultrasonication. This shear force and cavitation increases the inter-layer distance between MoS_2 layers, particularly to the end of bulk crystal, once a space or gap is formed. As, the distance between the inter-layer is increased, the molecules of Triton X-100 enter between the layers and get adsorbed on the surface of MoS_2 layer.[7,10,18] The dispersion of MoS_2 with Triton X-100 is stabilized by the hydrophilic and hydrophobic interactions. The hydrophobic 4-(1,13,3- tetramethyl butyl)-phenyl / hydrocarbon end of Triton X-100 adhere to the surface of MoS_2, reducing the interfacial tension between MoS_2 and the solvent, where steric force plays an important role while the hydrophilic polyethylene oxide chain which are exposed to DI water, help to stabilize the dispersion by electrostatic repulsions. The interaction of MoS_2 with Triton X-100 facilitates ultrasonic exfoliation of MoS_2 preventing its agglomeration. The photographs of bulk MoS_2 powder and chemically exfoliated as-synthesized MoS_2 dispersed in DI water are shown in Figure S1 (see supporting information).

The XRD pattern of as-synthesized exfoliated MoS_2 nanosheets (named as M1 optimized sample; details described in method section) is shown in Figure 2a. The vertical tick marks below the XRD pattern shows the positions of the Bragg peaks and corresponding JCPDS No. 37–1492 for hexagonal structure of MoS_2. The lattice parameters were estimated from experimentally observed d values and indexed (hkl) plane through a computer program based least square fitting method using "unit cell refinement software." The estimated lattice parameters $a = b = 3.1689 \pm 0.0618$ Å, $c = 12.9417 \pm 0.1312$ Å are comparable to the standard lattice parameters $a = b = 3.16$ Å and $c = 12.29$ Å. The position and intensity of the (002) peak originating from the hexagonal MoS_2 can be used to judge the extent of exfoliation. The schematic of MoS_2 is a layered arrangement of S and Mo atoms (chalcogen atoms are in orange and transition metal are in blue color), as shown in inset of Figure 2a. The XRD spectrum of MoS_2 bulk powder and XRD spectra of MoS_2 bulk powder with exfoliated MoS_2 nanosheets are given in Figure S2a-b (see supporting information). This detectable diffraction peak observed at 14.46° is corresponding to the *c*-plane of stacking MoS_2 indicating expansion of the lattice along the c-axis and formation of stoichiometric ternary compounds. The inset of Figure S2b shows the enlarge view of major XRD peak (002), that is shifted towards the lower angle for exfoliated MoS_2 nanosheets in comparison to MoS_2 bulk powder sample. The peak shifting value is around 0.06° (see supporting information Figure S2b). The bulk unit cell of MoS_2 is also shown in inset of Figure S2a.

Raman spectroscopy is a non-destructive method to unambiguously pinpoint the number of sheets of the 2D layered TMDs. In order to examine the complete removal of Triton X-100 from the exfoliated MoS_2 nanosheets, we performed the Raman spectroscopy of pure Triton X- 100,

which was used as a medium of chemical exfoliation. It is clearly evident from the comparative studies of Raman spectra of exfoliated MoS_2 and Triton X-100 (Figure S3 see supporting information) that exhibit the presence of only peaks of MoS_2 in Raman spectrum of as-synthesized exfoliated MoS_2 nanosheets. Additionally no other peaks were observed, which confirms that the solvent has been completely removed after exfoliation of MoS_2. Thus, the Raman spectra provides the evidence that the exfoliated MoS_2 are completely Triton X-100 solvent-free. The Triton X-100 surfactant plays an important role in stabilizing the MoS_2 layers without incorporating on the surface. The MoS_2 nanosheets are stable even after removal of surfactant. While the MoS_2 nanosheets were sonicated with the surfactant, the surfactant separated the MoS_2 nanosheets by increasing the d-spacing between the p_z orbitals of MoS_2. This d-spacing is sustained until unless some external forces act upon it. Additionally, the Raman spectra of bulk MOS_2 (blue curve) and as-synthesized M1 sample (black curve) is also shown in Figure S3 (see supporting information) to prove that our as-synthesized sample converts from bulk into few layer after exfoliation. The E^1_{2g} (384.1 cm^{-1}) and A_{1g} (408.9 cm^{-1}) modes of Raman vibrations are represented for bulk MoS_2 and E^1_{2g} (383 cm^{-1}) and A_{1g} (408 cm^{-1}) modes of Raman vibrations are obtained for MoS_2 nanosheets. It means that there is a slight blue shift ($E^1_{2g} \sim 1.1$ cm^{-1} and $A_{1g} \sim 0.9$ cm^{-1}). This difference is due to the inter-planer restoring force which increases in bulk case. The enlarge view of Raman spectrum of as-synthesized M1 is shown in Figure 2b.

These two major peaks at 383 cm^{-1} and 408 cm^{-1} are representing the Raman frequencies of in-plane vibrational mode of the Mo and S atoms (E^1_{2g} modes) and the out-of-plane vibrational mode of S atoms (A_{1g} modes), respectively.[19,20] It is well established in recently published literature, which clearly shows that seven to eight layers are obtained at E^1_{2g} (383 cm^{-1}) and A_{1g} (408 cm^{-1}) modes of vibration.[21–25] Thus, this result indicates that the as-synthesized MoS_2 nanosheets were mainly composed of seven to eight layers. The optical image, optical profile and corresponding Raman mapping of as synthesized M1 sample are shown in Figure 2c-e. The optical depth profile signifies the excellent depth resolution, intensity and features the generation of Raman mapping of the as-synthesized MoS_2 nanosheets. The Raman mapping of the integrated intensity of the E_{2g} and A_{1g} is showing bright contrast (Figure 2e). The depth profile (Figure 2d) and Raman mapping (Figure 2e) were recorded at spots indicated by red colored straight line and blue colored square in Figure 2c, respectively. The range has been taken for the Raman mapping within the area of E^1_{2g} and A_{1g} that has the centred peak at 383 cm^{-1} and 408 cm^{-1}, respectively. The FTIR spectrum of as-synthesized M1 sample is given in Figure S4 (see supporting information). The peak around 3331 cm^{-1} is ascribed to the stretching of hydroxyl group.

X-ray photoelectron spectroscopy (XPS) was carried out to determine the chemical purity and composition of the as-synthesized exfoliated MoS_2 nanosheets using Triton X-100 surfactant. The XPS studies of the MoS_2 nanosheets has been performed after the complete removable of surfactant by repeated washing. The survey scan of exfoliated MoS_2 nanosheets is shown in Figure 3a, representing the Mo 3d and S 2p regions.

A detailed study on the bonding structure of the MoS_2 nanosheets was made using XPS Mo 3d and S 2p profiles, which are de-convoluted by Gaussian fitting to get information about bonding characteristics. At room temperature, the significant peaks present binding energies at 229 eV, 232 eV, 163 eV and 1324 eV correspond to the Mo $3d_{5/2}$, Mo $3d_{3/2}$, S 2p and S 2p, respectively (Figure 3b-d). The core level peaks in Figure 3b-d further suggest that the stoichiometric structure and phase composition of the MoS_2 nanosheets mostly remained unchanged. These results are consistent with the reported data of MoS_2, implying that the obtained MoS_2 nanosheets mainly have hexagonal phase.

The thickness of the exfoliated sheets is determined by atomic force microscopy (AFM) (see supporting information Figure S5). The surface morphology was very smooth and its root-mean-square (RMS) roughness values were less than 0.3 nm even in the 40 μm line profiles, indicating atomically flat MoS_2 nanosheets (Figure S5a,b). A black bold line peak to peak on the AFM image is shown (Figure S5b), where the step height was estimated. The exfoliated MoS_2 sheets were found to be 300–800 nm in lateral dimensions and exhibited typical total thickness around 8–10 nm, as shown in inset of Figure S5b. The total thickness estimated for 10 different samples synthesized by same technique is also shown in figure S6 (see supporting information). It also confirmed that thickness of exfoliated MoS_2 nanosheets is in the range of 8–10 nm.

The uniformity and size distribution of the as-synthesized M1 sample are also examined using scanning electron microscopy (SEM) (Figure 4a,b). One significant result shows exfoliated, 2D randomly oriented sub-micrometer sized nanosheets of irregular shape. This is clearly visible in the magnified view of panel a, as shown in Figure 4b. Transmission electron microscopy (TEM) was performed to analyze the existence of the majority of exfoliated 2D nanosheets in dispersion solution of as-synthesized M1 sample suspended on a copper coated carbon TEM grid (Figure 4c-d). The exfoliated MoS_2 are nearly transparent nanosheets with partial overlaps, as shown by the yellow marked arrows (Figure 4c). It exhibits a continuous film on the TEM grids. The edge folding is a common phenomenon in two-dimensional materials to determine the number of layers. It means that the single dark line at the folded edge could be correlated to a monolayer.[8] A magnified view of the cross sectional TEM image is given in Figure 4d. The lateral size of these sheets was typically a few hundred nanometers in length. It clearly depicted that a number of folded edges with multi-parallel lines corresponding to seven or eight layers of MoS_2 are observed. It asserts its layered structure with thickness in a range of ~1-1.5 nm. It is also directly related to the atomic number of the atoms imaged, allowing atom-by-atom chemical identification. The SEM, TEM, HRTEM and SAED pattern of bulk MoS_2 powder sample are shown in Figure S7 (see supporting information).

The typical UV-Vis absorption spectra of bulk MoS_2, chemically exfoliated as-synthesized M1 sample and Triton X-100

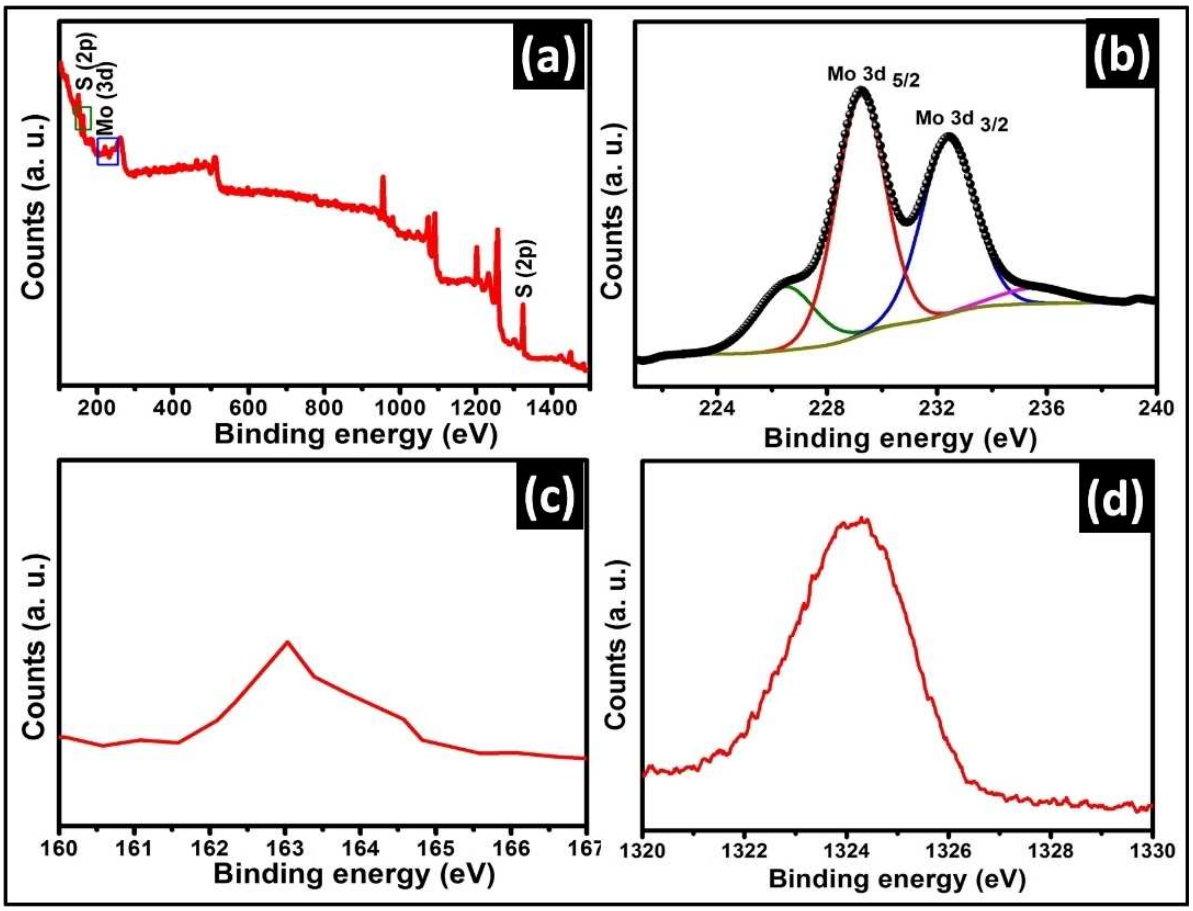

Figure 3. (a) XPS spectrum of as-synthesized M1 sample, (b) enlarge view of panel a having high resolution spectra of core level peak of Mo ; Mo 3d peaks with peak position and width characteristic of the 2H phase, (c) and (d) enlarge view of panel a having core level peak of S.

surfactant is shown in Figure S8a (see supporting information). As-synthesized nanosheets exhibit no clear characteristic peaks of pristine MoS_2 except for the high energy excitonic features in the near-UV range. The absorption spectrum of chemically exfoliated MoS_2 shows peaks at 300, 395, 451, 614 and 674 nm. The peaks at 614 and 674 nm are ascribed to the characteristic A_1 and B_1 direct excitonic band gap transitions at K point, with the energy split from valence band spin-orbital coupling.

The estimated optical band gap of chemically exfoliated as-synthesized M1 sample using the UV-Vis absorption spectra is approximately 1.79 eV, calculated by tauc plot, as shown in Figure S8b (see supporting information). It concludes the semiconducting property preserve after chemical exfoliation of MoS_2 using Triton X-100 surfactant.

The PL emission spectra of MoS_2 bulk powder and exfoliated as-synthesized MoS_2 nanosheets using Triton X-100 surfactant solution having various quantity of MoS_2 is shown in Figure S9a. It was observed that dispersion of 0.3 gm of MoS_2 bulk powder in Triton X-100 is the best for exfoliation into MoS_2 nanosheets having highest PL intensity. The PL emission spectra of exfoliated MoS_2 for different sonication time interval are shown in Figure S9b. It shows that the best sonication time is 4 hours, which has highest PL intensity. Thus, the optimized sample 0.3 gm of MoS_2 powder having 4 hours sonication time is best for synthesis of the high luminescence nanosheets. The PLE and PL spectrum of bulk MoS_2 powder (black curve) and as-synthesized exfoliated MoS_2 nanosheets (red curve, M1 sample) are shown in Figure 5a,b, respectively. The PLE spectrum shows a shoulder peak at 518 nm, under emission wavelength of 664 nm (Figure 5a). The exfoliated MoS_2 nanosheets exhibits a stronger PL emission compared to bulk MoS_2 due to the change in band gap (Figure 5b).

The Figure 5b shows a broad peak centred at 664 nm upon excited at 518 nm, which is associated with excitonic peak arising from the K point of the Brillouin zone.[2,27] The luminescence is absent in the bulk MoS_2 sample having indirect bandgap. The PL enhancement is due to the quantum confinement effect in exfoliated few layer nanosheets. Basically, when the exfoliation of nanosheets from bulk occurs, the band gap starts to change from particular thickness and sharply goes to confinement region.

However, the full change in indirect to direct band gap appears in single layer. The band gap of synthesized sample approaches towards the region of direct band gap. The recently published literature confirms the similar explanation.[2] Therefore, the stronger emission is observed in exfoliated nanosheets

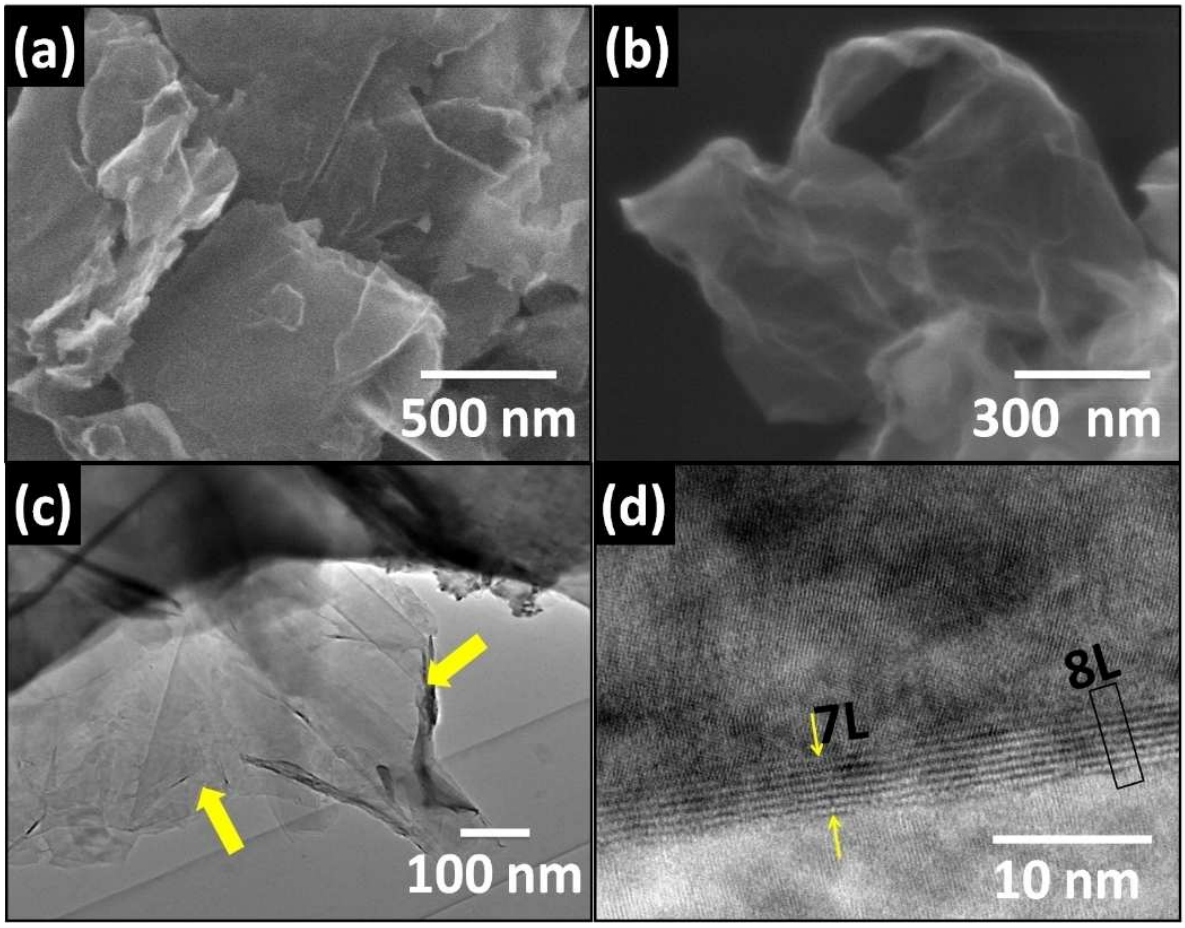

Figure 4. (a) SEM image of as-synthesized M1 sample, (b) magnified view of panel a, (c) cross-sectional TEM images of as-synthesized M1 sample; the chemically exfoliated MoS_2 image clearly demonstrates are nearly transparent nanosheets with partial overlaps, (d) magnified view of the cross sectional TEM image of panel c; consisting of seven-eight layers of MoS_2; folded edge of MoS_2 layer with continually dark line contrast alignment change at the edge.

as compared to bulk from less than 1% (bulk) to over 82% (MoS_2 nanosheets) in a single stage, when Triton X-100 is used as a non-ionic surfactant for chemical exfoliation. This optical PL enchancement proceeds in a single stage whereas other reported paper show some treatment method required for enhancing PL of 2D materials, which is a cumbersome process.[28,29] The kinetic theory is developed of luminescence quenching in the presence of migration of the excitations over the donors. The kinetics of the luminescence damping is determined in the entire time scale. It is obtained for the rate of luminescence quenching for an arbitrary multipole interaction of the donors with the acceptors.[30,31] The kinetics of Integrated PL intensity is also calculated for different period of time (Figure S10; see supporting information). The intensity is approximately same all over the periods. It confirms that the uniform sample can be synthesized by this method. Therefore, the above Raman and PL results qualitatively specify the formation of MoS_2 nanosheets by surfactant assisted exfoliation. The CIE color co-ordinates (chromaticity diagram) obtained from emission spectra are $x = 0.7128$ and $y = 0.2872$, as shown in inset of Figure 5b and located typically in the red region. However, the time-dependent process of energy transfer of as-synthesized exfoliated MoS_2 is also desirable, which can be correspondingly obtained from the kinetics of the luminescence, which is presented in Figure 5c,d. The radiative transition is observed at 664 nm emission at 375 nm picoseconds diode laser and the decay profile is shown in Figure 5c. Figure 5d demonstrates the exponential fitting of decay profiles and the corresponding parameters generated from fitting are listed in inset of Figure 5d. The decay profile of exfoliated MoS_2 is fitted and displays a nearly double exponential behavior convoluted with the instrument response function of the detector, as shown in equation (1), where τ_1 and τ_2 are the decay lifetimes of the luminescence, and A_1 and A_2 are the weighting parameters.

$$I(t) = A_1 \exp(-t/\tau_1) + A_2 \exp(-t/\tau_2) \quad (1)$$

The observed parameters are $\tau_1 = 0.4039$ ns, $\tau_2 = 2.147$ ns, $\chi 2 = 1.21$, $A_1 = 0.604$ and $A_2 = 0.396$. The results indicates the presence of two electronically excited species which have faster and slower lifetimes. The average lifetime for luminescent as-synthesized sample is $\tau_{av} = 1.81$ ns, which is calculated using equation (2).

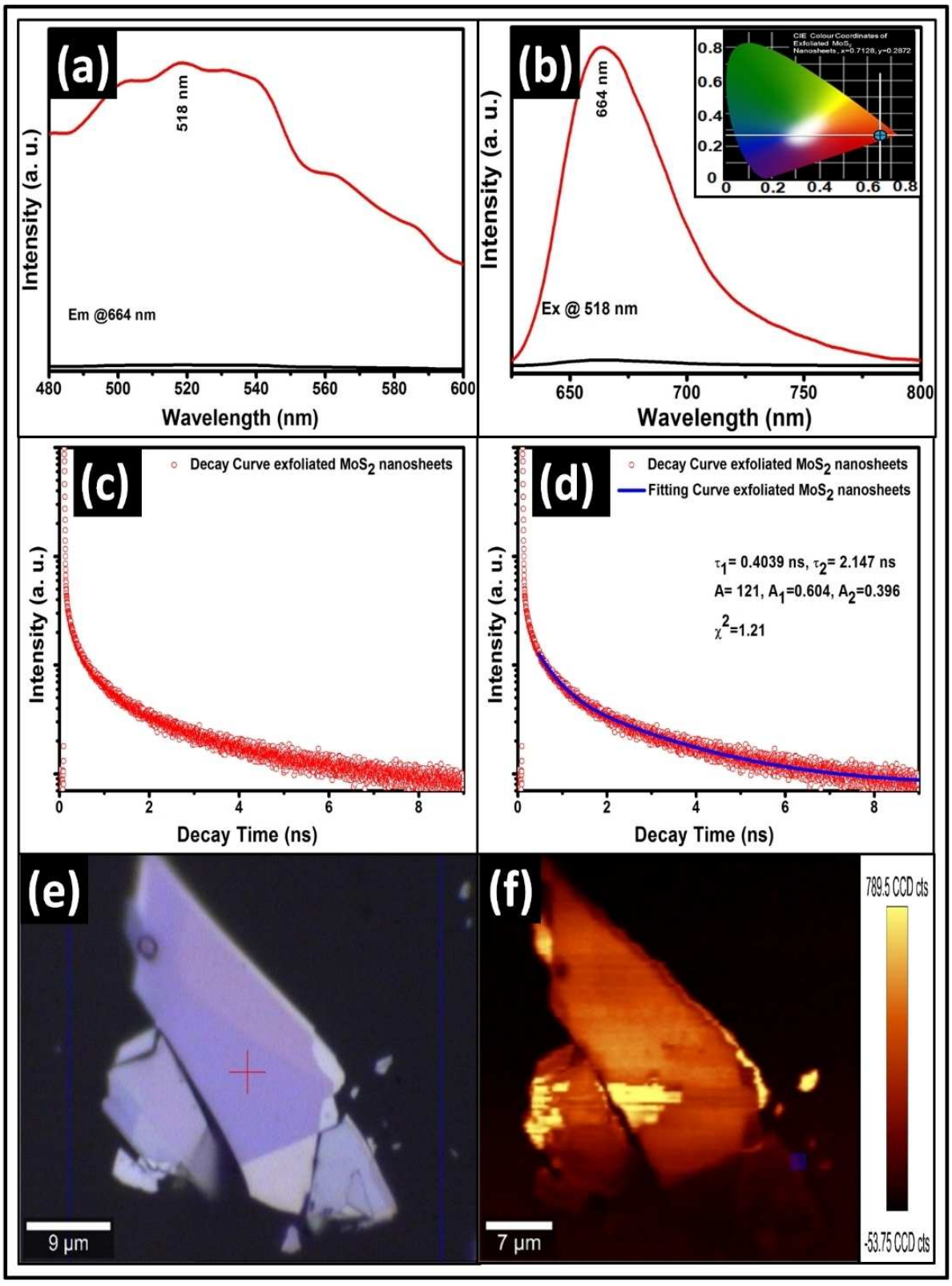

Figure 5. (a) Excitation spectrum of the as-synthesized M1 sample at 664 nm emission wavelength, (b) emission spectrum of the as-synthesized M1 sample at 518 nm excitation; inset shows the CIE co-ordinates from emission spectra of the as-synthesized M1 sample, (c) time resolved PL decay profiles as-synthesized M1 sample recorded at room temperature, (d) time-resolved photoluminescence decay spectra with a fitting curve and their corresponding lifetime data parameters generated by exponential fitting of the as-synthesized M1 sample and (e,f) the optical image and their corresponding PL mapping of as synthesized M1 sample; The PL spectrum (b) and PL mapping (f) were recorded at spots indicated by red colored crosses and blue colored square in (e), respectively.

$$\tau_{av} = (A_1\tau_1^2 + A_2\tau_2^2)/(A_1\tau_1 + A_2\tau_2) \quad (2)$$

The optical image and corresponding PL mapping of as synthesized M1 sample are shown in Figure 5e,f. The PL spectrum (Figure 5b) and PL mapping (Figure 5f) were recorded at spots indicated by red colored crosses and blue colored square in Figure 5e, respectively. It could be clearly evidenced that the nanosheet is nearly demonstrating spatial distribution with high thickness uniformity all over the surface of sample region. As the final note, the obtained results suggests that the Triton X-100 induced liquid exfoliation of MoS_2 bulk into nanosheets is a promising approach for producing 2D MoS_2 nanosheets in large scale for the development of practical optoelectronic devices.

Conclusion

A facile approach to chemically exfoliate MoS_2 into mono and few layer nanosheets using Triton X-100 in single stage is demonstrated. In this method, the exfoliated MoS_2 conserves its structure with pristine electronic properties and parallelly produces strong luminescence. In contrast to other exfoliation method, we observed that the interaction of Triton X-100 not only initiates the exfoliation process by increasing the exfoliation energies through hydrophilic repulsions between the Triton X-100 molecules but also increases the interlayer distance between the MoS_2 layers. The emerging photoluminescence results demonstrated that the exfoliated MoS_2 have strong emission centered at 664 nm at excitation wavelength of 518 nm with lifetime in nanosecond. The structural/microstructural and surface morphology images confirm the high quality exfoliation of MoS_2 from bulk into nanosheets. Furthermore, PL mapping confirms the spatial uniform PL intensity distribution of exfoliated MoS_2 which is further evident by Raman mapping technique. Thus, this innovative approach to chemically exfoliate MoS_2 through inexpensive Triton X-100 exfoliating agent offers a new alternative route to produce large scale high quality luminescent MoS_2 few layers of nanosheets at economic cost for next generation optoelectronic and other portable thin film based electronic devices.

Supporting Information Summary

Supporting information contains complete experimental procedure and details of characterization techniques. XRD, SEM, TEM, Raman, FTIR, AFM and PL.

Acknowledgements

The authors wish to thank Director, CSIR-NPL, New Delhi, for his keen interest in the work. The authors are thankful to Prof. O. N. Srivastava (Banaras Hindu University, Varanasi) for his encouragement. The authors are grateful to the CSIR-TAPSUN program for confocal PL mapping facility.

Conflict of Interest

The authors declare no conflict of interest.

Keywords: Metal dichalcogenides · molybdenum disulfide · 2D materials · photoluminescence · Raman microscopy

[1] S. Das, H.-Y. Chen, A. V. Penumatcha, J. Appenzeller, *Nano lett.* **2012**, *13*, 100–105.
[2] G. Eda, H. Yamaguchi, D. Voiry, T. Fujita, M. Chen, M. Chhowalla, *Nano lett.* **2011**, *11*, 5111–5116.
[3] Y. H. Lee, X. Q. Zhang, W. Zhang, M. T. Chang, C. T. Lin, K. D. Chang, Y. C. Yu, J. T. W. Wang, C. S. Chang, L. J. Li, *Adv. Mater.* **2012**, *24*, 2320–2325.
[4] Y. Huang, J. Wu, X. Xu, Y. Ho, G. Ni, Q. Zou, G. K. W. Koon, W. Zhao, A. C. Neto, G. Eda, *Nano Res.* **2013**, *6*, 200–207.
[5] J. Pu, Y. Yomogida, K.-K. Liu, L.-J. Li, Y. Iwasa, T. Takenobu, *Nano lett.* **2012**, *12*, 4013–4017.
[6] Y. Yoon, K. Ganapathi, S. Salahuddin, *Nano lett.* **2011**, *11*, 3768–3773.
[7] V. Nicolosi, M. Chhowalla, M. G. Kanatzidis, M. S. Strano, J. N. Coleman, *Science* **2013**, *340*, 1226419.
[8] U. Halim, C. R. Zheng, Y. Chen, Z. Lin, S. Jiang, R. Cheng, Y. Huang, X. Duan, *Nature commun.* **2013**, *4*, 2213.
[9] J. Shen, Y. He, J. Wu, C. Gao, K. Keyshar, X. Zhang, Y. Yang, M. Ye, R. Vajtai, J. Lou, *Nano lett.* **2015**, *15*, 5449–5454.
[10] J. N. Coleman, M. Lotya, A. O'Neill, S. D. Bergin, P. J. King, U. Khan, K. Young, A. Gaucher, S. De, R. J. Smith, *Science* **2011**, *331*, 568–571.
[11] H. Ramakrishna Matte, A. Gomathi, A. K. Manna, D. J. Late, R. Datta, S. K. Pati, C. Rao, *Angew. Chem. Int. Ed.* **2010**, *49*, 4059–4062.
[12] P. Joensen, R. Frindt, S. R. Morrison, *Mater. res. bull.* **1986**, *21*, 457–461.
[13] G. B. de-Mello, L. Smith, S. J. Rowley-Neale, J. Gruber, S. J. Hutton, C. E. Banks, *RSC Adv.* **2017**, *7*, 36208–36213.
[14] E. Varrla, C. Backes, K. R. Paton, A. Harvey, Z. Gholamvand, J. McCauley, J. N. Coleman, *Chem. Mater.* **2015**, *27*, 1129–1139.
[15] R. Giovannetti, E. Rommozzi, M. Zannotti, C. D'Amato, S. Ferraro, M. Cespi, G. Bonacucina, M. Minicucci, A. Di Cicco, *RSC Adv.* **2016**, *6*, 93048–93055.
[16] J. Bai, D. R. Soden, L. Dong, *ECS Trans.* **2014**, *61*, 3–8.
[17] L. O. Shyyko, V. O. Kotsyubynsky, I. M. Budzulyak, *J. Nanosci. Nanotech.* **2016**, *16*, 7792–7796.
[18] A. Ciesielski, P. Samorì, *Chem. Soc. Rev.* **2014**, *43*, 381–398.
[19] H. Wang, L. Yu, Y.-H. Lee, Y. Shi, A. Hsu, M. L. Chin, L.-J. Li, M. Dubey, J. Kong, T. Palacios, *Nano lett.* **2012**, *12*, 4674–4680.
[20] B. Cho, A. R. Kim, Y. Park, J. Yoon, Y.-J. Lee, S. Lee, T. J. Yoo, C. G. Kang, B. H. Lee, H. C. Ko, *ACS App. Mater. Inter.* **2015**, *7*, 2952–2959.
[21] B. Chakraborty, H. R. Matte, A. Sood, C. Rao, *J. Raman Spectro.* **2013**, *44*, 92–96.
[22] C. Rao, H. Ramakrishna Matte, U. Maitra, *Angew. Chem. Int. Ed.* **2013**, *52*, 13162–13185.
[23] C. Rao, U. Maitra, U. V. Waghmare, *Chem. Phys. Lett.* **2014**, *609*, 172–183.
[24] J.-U. Lee, M. Kim, H. Cheong, *Appl. Micro.* **2015**, *45*, 126–130.
[25] X.-L. Li, X.-F. Qiao, W.-P. Han, X. Zhang, Q.-H. Tan, T. Chen, P.-H. Tan, *Nanotech.* **2016**, *27*, 145704.
[26] S. Bai, L. Wang, X. Chen, J. Du, Y. Xiong, *Nano Res.* **2015**, *8*, 175–183.
[27] A. Splendiani, L. Sun, Y. Zhang, T. Li, J. Kim, C.-Y. Chim, G. Galli, F. Wang, *Nano lett.* **2010**, *10*, 1271–1275.
[28] J. H. Park, A. Sanne, Y. Guo, M. Amani, K. Zhang, H. C. P. Movva, J. A. Robinson, A. Javey, S. K. Banerjee, A. C. Kummel, *Science Adv.* **2017**, *3*, e1701661.
[29] M. Amani, P. Taheri, R. Addou, G. H. Ahn, D. Kiriya, D. H. Lien, J. W. Ager, R. M. Wallace, A. Javey, *Nano Lett.* **2016**, *16*, 2786–2791.
[30] L. Zusman, *Sov. Phys. JETP* **1977**, *46*, 347.
[31] R. A. Vilá, R. Rao, C. Muratore, E. Bianco, J. A. Robinson, B. Maruyama, N. R. Glavin, *2D Mater.* **2017**, *5*, 011009.

Submitted: April 11, 2019
Accepted: May 15, 2019